Appl. Phys. B 84, 433–438 (2006)
DOI: 10.1007/s00340-006-2270-6

Applied Physics B
Lasers and Optics

M. GAO✉
J. WANG
C. JIANG
W. HU
H. REN

Two-pump fiber optical parametric amplifiers using optimized photonic crystal fiber by genetic algorithm

State Key Laboratory of Advanced Optical Communication Systems & Networks,
Shanghai Jiao Tong University, Shanghai 200030, P.R. China

Received: 9 January 2006/Revised version: 7 April 2006
Published online: 31 May 2006 •

ABSTRACT In this paper, we investigate the gain spectra of fiber optical parametric amplifiers (FOPAs) consisting of dispersion-flattened fibers (DFFs) with different dispersion curves comparatively by means of the dispersion curve model of the DFFs. It is demonstrated that the broader gain spectrum of FOPAs can be achieved if the dispersion curve is lower and more flattened. Based on the preceding analyses, we propose to constitute FOPAs by using index-guiding photonic crystal fiber (PCF) with an anticipated ultra-flattened dispersion and ultra-low dispersion slope. The as-proposed PCF had different air-holes in the cladding rings. In total, four parameters of the PCF are optimized by using genetic algorithm.

PACS 42.81.-i; 42.65.Hw; 42.65.Yj

1 Introduction

In current communication systems, wavelength division multiplexing (WDM) is used to increase the information capacity of each fiber, which requires amplifiers with uniform gain to compensate the loss of fiber and equalize the power of the various channels. Fiber optical parametric amplifiers (FOPAs), which utilize the principle of four-wave mixing (FWM) to amplify the signals [1], can provide a broadband amplification at arbitrary wavelengths when the two pump wavelengths locate on each side of the zero-dispersion wavelength (ZDW) and the center wavelength of two pumps is close to ZDW [2–4].

In most research, the dispersion slope of fiber D_λ (that is $\partial D/\partial\lambda$) is considered as a constant and therefore the gain spectrum of FOPAs is nearly symmetrical [5–7]. However, in practice the dispersion of fiber $D(\lambda)$ varies with the wavelength, so does the dispersion slope $D_\lambda(\lambda)$. In this paper, we model the dispersion curve of DFF as a parabola and obtain its second- and fourth-order dispersion curves, from which the gain spectrum of FOPAs using DFF is achieved. Compared with the symmetrical gain spectrum in [8], the gain spectrum of FOPAs in the paper is asymmetrical because a varying dispersion slope of fiber with wavelength $D_\lambda(\lambda)$ is considered to substitute for a constant D_λ. The gain spectra of FOPAs with different dispersion curves are compared, and it is known that the lower and more flattened the dispersion curve is, the broader the gain spectrum is.

Based on preceding analyses, index-guiding photonic crystal fibers (PCFs) are proposed to constitute FOPAs [9, 10]. From the first time PCFs are used in FWM [11], the optical parametric oscillator composed of PCFs has been the hotspot in research [12–17]. In most research, the pump wavelength of the optical parametric oscillator ranges from 600 nm to 800 nm [11–14]: In 2003, John D. Harvey et al. reported a photonic crystal fiber-optica parametric generator providing efficient conversion of red pump light with the wavelength of 647 nm into bule and near-infrared light [12]; subsequently A. Chen et al. proposed a widely tunable optical parametric generation in a PCF with the pump wavelength of 650 nm and demonstrated experimentally more than 450 nm of side-band tunability when the pump wavelength was tuned over 10 nm [13], which has a striking advancement compared with the first PCF-optical parametric oscillator with the measured wavelength-tunability range of 40 nm in the case of pump wavelength of 751.8 nm [11]. Moveover, the FWM in PCF also was applied to generate femtosecond pulses: In 2004, S.O. Konorov et al. put forward a generator of femtosecond anti-Stokes pulses, which utilized 800 nm laser pump pulses into an anti-Stokes signal with the central wavelength around 590–600 nm and a Stokes signal centered at 1250 nm [14]; in 2005, Y. Deng et al. reported a broadly tunable femtosecond parametric oscillator using a PCF and achieved pulses as short as 460 fs and a tuning range as wide as 200 nm around 1000 nm with the pump wavelength of 1040 nm [15]. In recent research, the dispersion-flattened highly nonlinear PCF has been utilized in wavelength conversion in the range of communication wavelength: In 2005, P.A. Andersen et al. proposed a wavelength converter using dispersion-flattened highly nonlinear PCF and achieved a conversion bandwidth of 31 nm with a range of the pump wavelength from 1559.8 nm to 1545.2 nm [16]; K.K. Chow et al. also reported a polarization-insensitive widely tunable wavelength converter in dispersion-flattened nonlinear PCF and obtained a 3-dB conversion range over 40 nm (1535–1575 nm) with a flat conversion efficiency of −16 dB and a polarization sensitivity of less than 0.3 dB [17].

As is known, photonic crystal fibers (PCFs) are made from single material such as silica glass, with an array of micro-

✉ Fax: 86-21-62933306, E-mail: gmy@sjtu.edu.cn

scopic air channels running along its length [18]. A desirable property of the PCFs is that the additional design parameters of hole diameter, d, and hole pitch, Λ, offer much greater flexibility in the design of dispersion for the required application. By manipulating circular air-hole diameter, d, and pitch, Λ, it is possible to control the PCF dispersion properties, for example, to change the zero-dispersion wavelength or to engineer the dispersion curve to be ultra-flattened. The optimization design of PCFs is often difficult because the optical properties do not usually vary in a simple way with the fiber geometry parameters [19]. Therefore, optimization design is proposed to consider the problem inversely, i.e., designing the PCFs structure based on the anticipated optical characteristic for a given application. In the paper, based on the model of dispersion curve of fiber and the gain theory of FOPAs, the conclusion can be drawn that the lower and more flattened the dispersion curve of fiber is, the broader the gain spectrum of FOPAs is. Moreover, the chromatic dispersion of PCFs can be engineered easily by varying the holes' diameter and the holes' pitch. Furthermore, if each ring's air-holes in cladding can be designed, respectively, better performance can be expected in wide wavelength range [20]. Therefore, we proposed a dispersion-flattened PCFs with the expected dispersion characteristics adapted to FOPAs and then used genetic algorithm (GA) to optimize the four design parameters of PCFs, where each ring's air-holes in cladding are different. Thus an anticipated PCF with the ultra-flattened dispersion and ultra-low dispersion slope over wide wavelength range is obtained and a new FOPA composed of this PCF also is proposed with a flattened gain band over 50 nm.

2 The dispersion-flattened FOPAs

For FOPAs, a small dispersion slope of fiber D_λ can provide a broad and uniform gain spectrum. In previous FOPA experiments, the dispersion slope of fiber D_λ is considered as a constant, such as $0.07\,\mathrm{ps/(nm^2km)}$ in common dispersion-shifted fiber (DSF) and $0.03\,\mathrm{ps/(nm^2km)}$ in highly nonlinear fiber (HNLF) [21, 22]. However, the dispersion of fiber $D(\lambda)$ is commonly variable with the wavelength, so is the dispersion slope $D_\lambda(\lambda)$, which has an important influence on the gain spectrum of FOPAs. Therefore a dispersion-flattened fiber is proposed in the paper to apply to FOPAs to achieve a broad and uniform gain spectrum.

The dispersion curve of DFFs $D(\lambda)$ can be assumed to be a parabola [23],

$$D(\lambda) = D_\mathrm{e}\left[1 - \frac{(\lambda-\lambda_\mathrm{e})^2}{\lambda_\mathrm{z}^2}\right]$$

Where D_e is the minimal value of $D(\lambda)$ at the wavelength λ_e and $2\lambda_\mathrm{z}$ is the wavelength spacing between the two points of ZDW. In numerical simulation, the absolute value of D_e is assumed to be $0.15\,\mathrm{ps/nm/km}$, λ_e is $1732.5\,\mathrm{nm}$ and λ_z is $180\,\mathrm{nm}$. Figure 1a shows the characteristic of dispersion function of DFFs and it is clear that the fiber dispersion $D(\lambda)$ varies with wavelength.

Supposing that the pumps are much more intense than the signal and idler and they co-propagate in a lossless fiber, the theoretical gain spectrum of two-pump FOPAs at the output can be expressed as the form [8]:

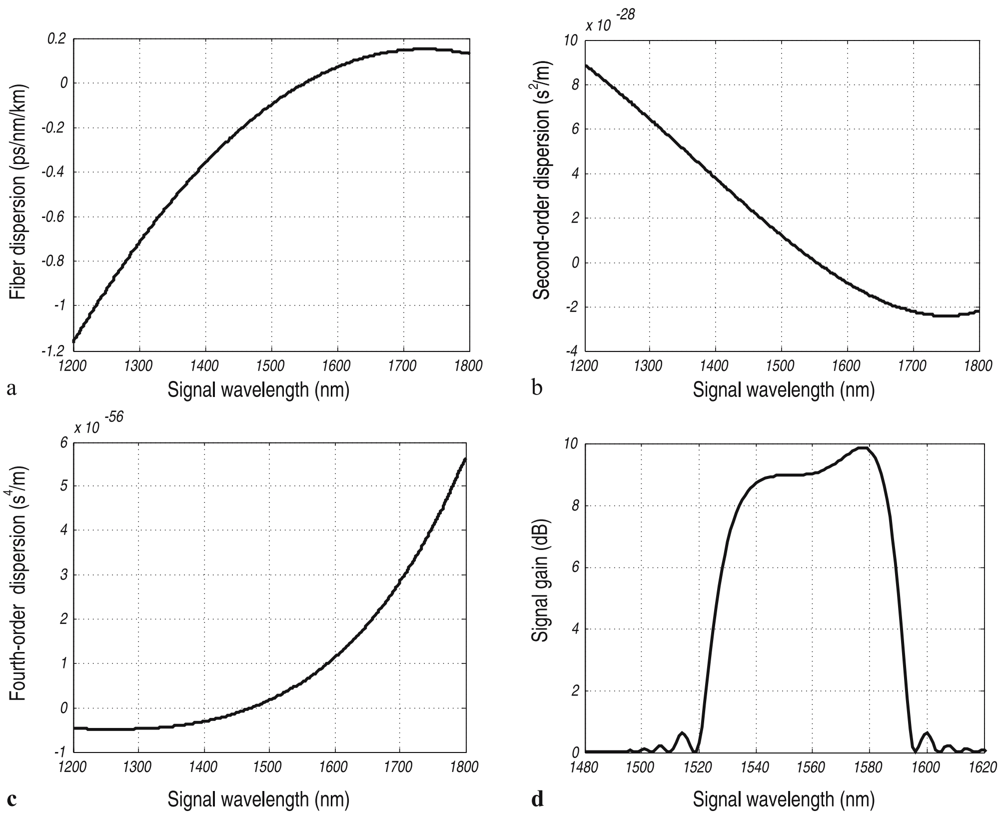

FIGURE 1 (**a**) The fiber dispersion D curve; (**b**) the second-order dispersion $\beta^{(2)}$ curve; (**c**) the fourth-order dispersion $\beta^{(4)}$ curve; (**d**) the signal gain G_s curve

$$G_s = 1 + \left[\frac{ur}{g}\sinh(gL)\right]^2 ,$$

where $u = \gamma(P_1 + P_2) = \gamma P_0$, $r = 2\sqrt{P_1 P_2}/P_0$, and the parametric gain coefficient g can be expressed:

$$g^2 = \left[(ur)^2 - (\kappa/2)^2\right] = -\frac{1}{4}(\Delta\beta^2 + 2u\Delta\beta + u^2 - 4u^2r^2) ,$$

where k is the total phase mismatch including the nonlinear phase shift:

$$k = \Delta\beta + \gamma(P_1 + P_2) = \Delta\beta + \gamma P_0 .$$

γ is the nonlinear coefficient of fiber and the linear propagation constant mismatch $\Delta\beta$ is shown:

$$\Delta\beta = \beta_3 + \beta_4 - \beta_1 - \beta_2 .$$

Define the parameters, the central frequency of the two pumps $\omega_c = (\omega_1 + \omega_2)/2$; the frequency detuning between the signal ω_3 and the central frequency $\Omega = \omega_3 - \omega_c$; the average difference of the two pumps' frequencies $\Delta\omega_p = (\omega_1 - \omega_2)/2$.

We expand β_3 around the central frequency of the two pumps ω_c:

$$\begin{aligned}\beta_3 &= \beta(\omega_c) + \frac{d\beta}{d\omega}(\omega_c)(\omega_3 - \omega_c) + \frac{1}{2}\frac{d^2\beta}{d\omega^2}(\omega_c)(\omega_3 - \omega_c)^2 \\ &\quad + \frac{1}{6}\frac{d^3\beta}{d\omega^3}(\omega_c)(\omega_3 - \omega_c)^3 + \cdots \\ &= \beta(\omega_c) + \sum_{n=1}^{\infty}\frac{\beta^{(n)}}{n!}(\omega_c)(\omega_3 - \omega_c)^n ,\end{aligned}$$

where $\beta^{(n)}$ denotes the nth derivative of β at ω_c. Similarly, we can write β_1, β_2 and β_4, and utilize the substitutions, $\Omega = \omega_3 - \omega_c = -(\omega_4 - \omega_c)$, $\Delta\omega_p = \omega_1 - \omega_c = -(\omega_2 - \omega_c)$.

The linear propagation-constant mismatch $\Delta\beta$ can be rewritten as:

$$\Delta\beta = 2\sum_{m=1}^{\infty}\frac{\beta^{(2m)}}{(2m)!}\left[\Omega^{2m} - (\Delta\omega_p)^{2m}\right] .$$

From [8], it is known that truncating $\Delta\beta$ after the fourth order should be a generally valid procedure and therefore $\Delta\beta$ can be expressed as following:

$$\Delta\beta = \beta^{(2)}\left[\Omega^2 - (\Delta\omega_p)^2\right] + \frac{1}{12}\beta^{(4)}\left[\Omega^4 - (\Delta\omega_p)^4\right] .$$

From the preceding theoretical analyses, it is clear that the dispersion characteristics govern the gain of FOPAs. Given a graph of fiber chromatic dispersion coefficient $D(\lambda)$, which is often available from manufacturers, the second and fourth derivation of β can be obtained [24]:

$$\begin{aligned}\beta^{(2)} &= -\frac{\lambda^2}{2\pi c}D , \\ \beta^{(4)} &= -\frac{\lambda^4}{8\pi^3c^3}\left(6D + 6\lambda\frac{\partial D}{\partial\lambda} + \lambda^2\frac{\partial^2 D}{\partial\lambda^2}\right) ,\end{aligned}$$

where D is the dispersion coefficient, $\partial D/\partial\lambda$ is the dispersion slope and $\partial^2 D/\partial\lambda^2$ is the second-order differential coefficient of dispersion. Figure 1b corresponds to $\beta^{(2)}$ and Fig. 1c corresponds to $\beta^{(4)}$. Thus the gain spectrum of two-pump FOPA

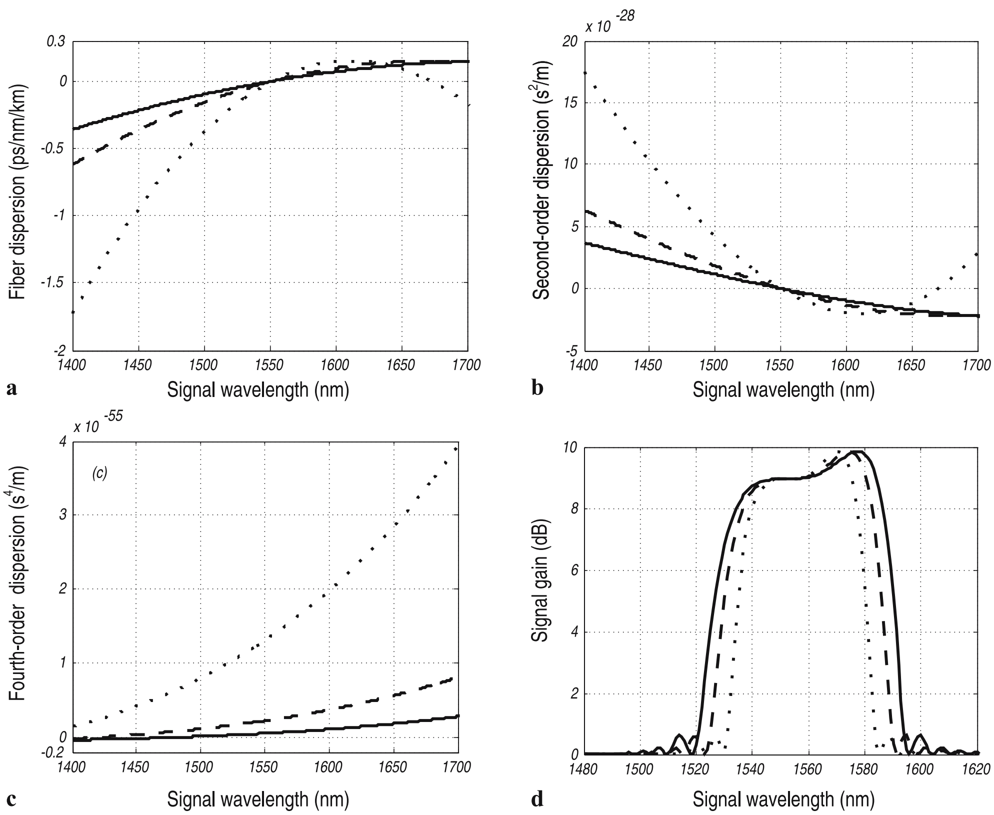

FIGURE 2 (**a**) The fiber dispersion D curves; (**b**) the second-order dispersion $\beta^{(2)}$ curves; (**c**) the fourth-order dispersion $\beta^{(4)}$ curves; (**d**) the signal gain G_s curves (the *dotted*, *dashed* and *solid line* denotes λ_z of 60, 120 and 180 nm, respectively)

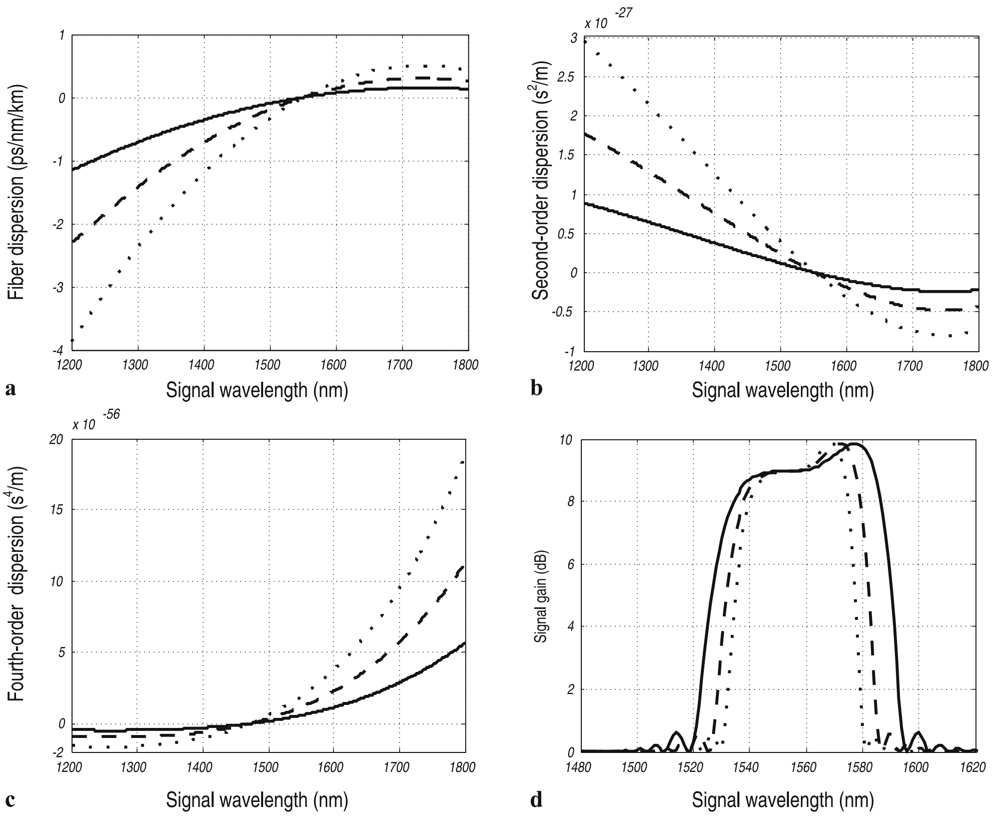

FIGURE 3 (**a**) The fiber dispersion D curves; (**b**) the second-order dispersion $\beta^{(2)}$ curves; (**c**) the fourth-order dispersion $\beta^{(4)}$ curves; (**d**) the signal gain G_s curves (the *dotted*, *dashed* and *solid line* denotes D_z of 0.5, 0.3 and 0.15 ps/nm/km, respectively)

can be obtained based on the dispersion curve $D(\lambda)$ in Fig. 1a, as shown in Fig. 1d. In numerical simulation, we consider a two-pump FOPA, which is assumed to use 100 m dispersion-flattened fiber with nonlinear coefficient of 18 W^{-1}/km, and pumped at 1553.1 nm and 1552 nm with a power of 0.5 W at each wavelength.

The value of $\beta^{(4)}$ is actually in a range from 10^{-6} to 10^{-4} ps^4/km. It has been known that the central wavelength of the two pumps should be tuned close to fiber ZDW in order to achieve a broad gain spectrum of FOPA [2], and hence the two pumps locate on each side of a ZDW of the fiber, in which case the effects of $\beta^{(4)}$ on the gain bandwidth cannot be neglected [25, 26]. As shown in [7], less the absolute value of $\beta^{(4)}$ is, larger the gain bandwidth becomes. Therefore it is feasible to design a fiber with lower value of $\beta^{(4)}$ to broaden the gain bandwidth of FOPAs.

From the preceding analyses, it is clear that the dispersion curve of fiber governs the gain spectrum of dispersion-flattened FOPAs. Therefore the parameters of dispersion curve are varied to find out their effects on gain spectrum. Firstly, it is evident that the variation of λ_e makes the gain spectrum move, but the figure doesn't change. Secondly, the wavelength spacing between the two points of ZDW $2\lambda_z$ is varied and the dispersion curves are shown in Fig. 2a–c. The corresponding gain spectra are gotten in Fig. 2d, and here λ_z is set to 60, 120 and 180 nm, respectively. Finally, the maximum value D_e of $D(\lambda)$ at the wavelength λ_e are assumed to be 0.15, 0.3 and 0.5 ps/nm/km, and the dispersion curves are shown in Fig. 3a–c. The corresponding gain spectra are shown in Fig. 3d and here λ_z is set to 180 nm in advance. From the Figs. 2 and 3, it is known that lower and more flattened the dispersion curve is, broader the gain spectrum of FOPAs is. Therefore, the next step we will perform is to design a PCF with the above dispersion performance.

3 The optimization design of PCFs using GA

Based on preceding analyses, we will design an index-guiding PCF, exhibiting ultra-flattened dispersion and ultra-low dispersion slope over wide wavelength range, to constitute FOPAs.

A desirable property of PCFs is that the additional design parameters of hole diameter, d, and hole pitch, Λ, offer much greater flexibility in the design of dispersion to get the required application, as shown in Fig. 4a. By manipulating circular air-hole diameter, d, and pitch, Λ, it is possible to control the PCFs' dispersion properties, for example, to change the ZDW or engineer the dispersion curve to be ultra-flattened [20, 27]. Furthermore, the diameters of different rings' air-holes around the core can be designed respectively in order to get more flattened dispersion curve [28, 29]. Based on this principle, a triangular PCF with flattened dispersion curve is designed, where diameters of two central rings' air holes d_1 and d_2 are different from the other air holes diameter d, as shown in Fig. 4b.

Full-vector finite element method (FEM) is applied to analyze the dispersion property of the PCF in the paper [30]. The effective refractive index of the fundamental mode is given by $n_{\text{eff}} = \beta/k_0$, β is the propagation constant, $k_0 = 2\pi/\lambda$ is the free-space wave number. Once the modal effective indices n_{eff} are solved, the dispersion parameter D can be obtained by:

$$D(\lambda) = -(\lambda/c)(\mathrm{d}^2 n_{\text{eff}}/\mathrm{d}\lambda^2)\,,$$

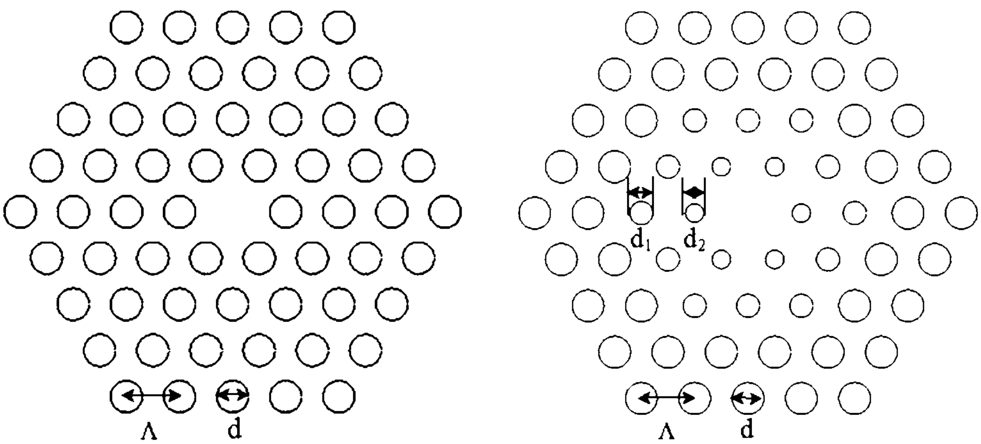

FIGURE 4 (**a**) Cross section of the triangular PCF with hole diameter d, pitch Λ; (**b**) cross section of the index-guiding PCF with hole diameter d, pitch Λ, where diameters of two central rings' air holes are d_1 and d_2

where c is the velocity of the light in a vacuum and λ is the operating wavelength. The four parameters Λ, d_1, d_2 and d can be optimized and more flattened dispersion curve from wavelength 1.4 μm to 1.7 μm, which is applied to FOPAs, can be obtained. And the GA is compatible in this process.

The genetic algorithm (GA), a multivariate stochastic optimization algorithm, is proposed in the paper to design dispersion-flattened PCFs. GAs were first introduced by Holland in 1975 [31, 32]. They are now applied to several fields in physics for which the resolution of inverse problem is needed [7].

The use of a GA requires the determination of six fundamental issues: the chromosome representation, the creation of the initial population, the fitness function, the selection function, the genetic operators making up the reproduction function and the termination criteria.

For any GA, an "individual" is a feasible solution that is described by a coded datum called a "chromosome" with values within the variables upper and lower bounds. In the paper, "chromosome" is described by $\{\Lambda, d_1, d_2, d\}$, where Λ is the holes' pitch and d_1, d_2, d are air-holes' diameters of different layers, respectively, as shown in the Fig. 4. And the initial population is set to 20 (popsize = 20) at the first generation. The fitness function F_j is defined to represent the degree of satisfaction of the dispersion performance.

$$F_j = \sum_{m=1}^{k} \left| D_{j,m} \right| ,$$

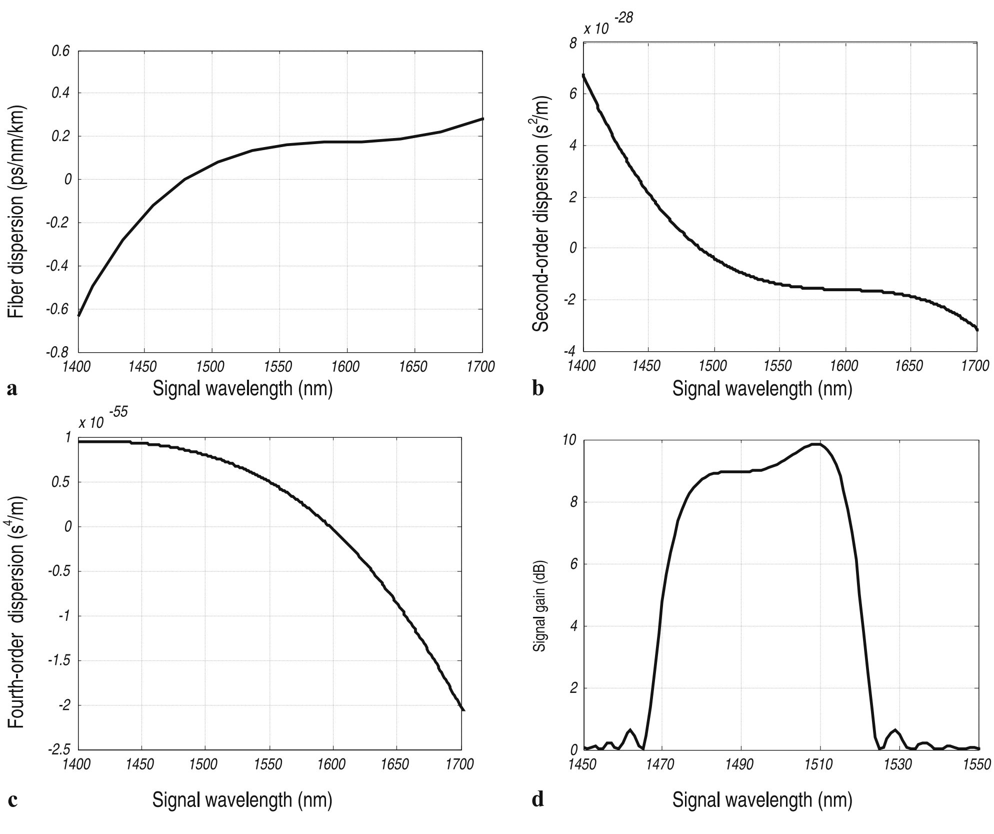

FIGURE 5 (**a**) The dispersion D curve of optimized index-guiding PCF with $\Lambda = 2.3$ μm, $d = 0.6394$ μm, $d_1 = 0.625$ μm, $d_2 = 0.55$ μm; (**b**) the corresponding second-order dispersion $\beta^{(2)}$ curve; (**c**) the corresponding fourth-order dispersion $\beta^{(4)}$ curve; (**d**) the signal gain G_s curve of FOPA using the optimized index-guiding dispersion-flattened PCF

where, k is the number of samples of the dispersion value from wavelength 1.4 μm to 1.7 μm and is fixed at 20 in the calculation, and dispersion function D_j is one of the solution solved from GA, $j = 1, 2, ...,$ popsize. Genetic operators provide the basic search mechanism of the GA: crossover and mutation, which are implemented at each generation. The operators are used to create new solution based on existing solutions in the population. The crossover rate here is 85% and the mutation rate is changed during the evolution process and initially it is set to be about 8%. The GA moves from generation to generation selecting and reproducing parents until a termination criterion is satisfied. The termination criterion is a specified maximum number of generations in our simulation and the number of generations is fixed at 50.

Finally, a PCF with low and flattened dispersion from wavelength of 1.4 μm to 1.7 μm, is obtained whose dispersion curves are shown in Fig. 5. As mentioned above, the fitness value F is used to evaluate the degree of satisfaction of the dispersion performance. And $F = 0$ corresponds to the ideal solution in this case. The GA optimizes the design process and improves the dispersion performance, which is expected to be more flattened in this case. In fact, dispersion values in the range of ± 0.2 ps/nm/km can be obtained from wavelength of 1.445 μm to 1.65 μm when parameters are set $\Lambda = 2.3$ μm, $d = 0.6394$ μm, $d_1 = 0.625$ μm and $d_2 = 0.55$ μm, which are the best solve of the last generation. Furthermore, we get the second-order dispersion $\beta^{(2)}$ between $\pm 2 \times 10^{-28}\ \mathrm{s^2/m}$ from the wavelength of 1450 nm to 1650 nm, as shown in Fig. 5b. However, the fourth-order dispersion $\beta^{(4)}$ needs the further improvement, which limits the gain bandwidth of the flattened gain of FOPAs.

In numerical simulation, the nonlinear coefficient of fiber is calculated by $\gamma = n_2\omega/(cA_{\mathrm{eff}})$ [33], where $n_2 = 2.45 \times 10^{-20}\ \mathrm{m^2/W}$ is the nonlinear-index coefficient, ω is the optical angular frequency, c is the velocity of light and $A_{\mathrm{eff}} = 5.52\ \mu\mathrm{m}^2$ is the effective mode area. And the other parameters are same as used in Fig. 2. Figure 5d shows the corresponding gain spectrum of FOPA using the designed PCF, which provides a gain of 10 dB over 50-nm bandwidth. It is evident that compared with Fig. 2d, the anticipated gain spectrum of FOPA has been obtained due to the application of PCF with ultra-flattened dispersion and ultra-low dispersion slope over a wide wavelength range, which is optimized by using GA.

4 Conclusion

In the paper, based on the dispersion curve of DFF modeled as a parabola, the gain spectrum of dispersion-flattened FOPAs is investigated, whose asymmetrical characteristic derives from that a varying dispersion slope of fiber with wavelength $D_\lambda(\lambda)$ is considered to substitute for a constant D_λ. The gain spectra of FOPAs consisting of DFF with different dispersion curves are compared and it is evident that lower and more flattened the dispersion curve of DFF is, broader the gain spectrum of FOPAs is. Subsequently, based on the above dispersion properties, the index-guiding PCF is engineered in full-vector finite element method, whose design parameters (Λ, d_1, d_2 and d) are optimized by using GA. A novel FOPA composed of the PCF with ultra-flattened dispersion and ultra-low dispersion slope over a wide wavelength range is obtained. In future research, we will focus on the improvement of the fourth-order dispersion by using GA.

ACKNOWLEDGEMENTS This work is supported in National Nature Science Foundation of China (Grant No. 60377023 and 90304002), the 863 Program and New Century Excellent Talents of Universities (NCET), Shanghai Optical Science and Technology Project.

REFERENCES

1 R.H. Stolen, J.E. Bjorkholm, IEEE J. Quantum Electron. **QE-18**, 1062 (1982)
2 C.J. Mckinstrie, S. Radic, A.R. Chraplyvy, IEEE J. Sel. Top. Quantum Electron. **8**, 538 (2002)
3 J.M. Chavez Boggio, J.D. Marconi, H.L. Fragnito, IEEE Photon. Technol. Lett. **17**, 1842 (2005)
4 F. Yaman, Q. Lin, S. Radic, G.P. Agrawal, IEEE Photon. Technol. Lett. **16**, 1292 (2004)
5 J. Hansryd, P.A. Andrekson, M. Westlund, J. Li, P.-O. Hedekvist, IEEE J. Sel. Top. Quantum Electron. **8**, 506 (2002)
6 M. Gao, C. Jiang, W. Hu, J. Wang, H. Ren, Opt. Commun. **258**, 321 (2006)
7 M. Gao, C. Jiang, W. Hu, J. Wang, Opt. Express **12**, 5603 (2004)
8 M.E. Marhic, Y. Park, F.S. Yang, L.G. Kazovsky, Opt. Lett. **21**, 1354 (1996)
9 R. Tang, J. Lasri, P. Devgan, J.E. Sharping, P. Kumar, Electron. Lett. **39**, 195 (2003)
10 F. Poli, F. Adami, M. Foroni, L. Rosa, A. Cucinotta, S. Selleri, Appl. Phys. B **81**, 251 (2005)
11 J. Sharping, M. Fiorentino, P. Kumar, R. Windeler, Opt. Lett. **27**, 1675 (2002)
12 J. Harvey, R. Leonhardt, S. Coen, G. Wong, J. Knight, W. Wadsworth, P.S.J. Russell, Opt. Lett. **28**, 2225 (2003)
13 A. Chen, G. Wong, S. Murdoch, R. Leonhardt, J. Harvey, J. Knight, W. Wadsworth, P. Russell, Opt. Lett. **30**, 762 (2005)
14 S.O. Konorov, E.E. Serebryannikov, A.M. Zheltikov, P. Zhou, A.P. Tarasevitch, D. von der Linde, Opt. Lett. **29**, 1545 (2004)
15 Y. Deng, Q. Lin, F. Lu, G. Agrawal, W. Knox, Opt. Lett. **30**, 1234 (2005)
16 P.A. Andersen, T. Tokle, Y. Geng, C. Peucheret, P. Jeppesen, Photon. Technol. Lett. **17**, 1908 (2005)
17 K.K. Chow, C. Shu, C.L. Lin, A. Bjarklev, IEEE Photon. Technol. Lett. **17**, 624 (2005)
18 T.-L. Wu, C.-H. Chao, IEEE Photon. Technol. Lett. **17**, 67 (2005)
19 E. Kerrinckx, L. Bigot, M. Douay, Y. Quiquempois, Opt. Express **12**, 1990 (2004)
20 K. Saitoh, M. Koshiba, Opt. Express **11**, 843 (2003)
21 J. Kim, Ö. Boyraz, J.H. Lim, M.N. Islam, IEEE J. Lightwave Technol. **19**, 247 (2001)
22 K.K.Y. Wong, K. Shimizu, K. Uesaka, G. Kalogerakis, M.E. Marhic, L.G. Kazovsky, IEEE Photon. Technol. Lett. **15**, 1707 (2003)
23 M. Yu, C.J. McKinstrie, G.P. Agrawal, Phys. Rev. E **52**, 1072 (1995)
24 M.-C. Ho, K. Uesaka, M. Marhic, Y. Akasaka, L.G. Kazovsky, IEEE J. Lightwave Technol. **19**, 977 (2001)
25 M.E. Marhic, N. Kagi, T.-K. Chiang, L.G. Kazovsky, Opt. Lett. **21**, 573 (1996)
26 K. Inoue, IEEE J. Lightwave Technol. **10**, 1553 (1992)
27 W.H. Reeves, J.C. Knight, P.S.J. Russell, Opt. Express **10**, 609 (2002)
28 F. Poli, A. Cucinotta, S. Selleri, A.H. Bouk, IEEE Photon. Technol. Lett. **16**, 1065 (2004)
29 K. Saitoh, M. Koshiba, Opt. Express **11**, 3100 (2003)
30 T.-L. Wu, C.-H. Chao, IEEE Photon. Technol. Lett. **16**, 126 (2004)
31 J.H. Holland, *Adaptation in Natural and Artificial Systems* (The M.I.T. Press, Cambridge, MA, 1975)
32 D.E. Goldberg, *Genetic Algorithms in Search, Optimization, and Machine Learning* (Addison-Wesley, New York, 1989)
33 G.P. Agrawal, *Nonlinear Fiber Optics, Third Edition & Applications of Nonlinear Fiber Optics* (Publishing House of Electronics Industry, Beijing, 2002)